Optimizing Heat Transfer in Heat Sink Fin Arrays Using Computational Fluid Dynamics

MCEN 4231/5231 Term Project
Department of Mechanical Engineering
University of Colorado Boulder

Submitted by: Surya Sharon Raj Goda, Saravana Kumar Kodakinti Prakash,
Anoop Subramanya, K. Vaikunth Keshav
Date: May 6, 2025

Abstract

This study investigates the optimal fin configuration for passive heat sinks using computational fluid dynamics (CFD). Natural convection heat transfer was simulated in three different fin array configurations (6, 10, and 13 fins) to determine the optimal spacing that maximizes heat transfer while minimizing material usage. A monolithic coupling approach with the Boussinesq approximation was employed to solve the coupled Navier-Stokes and energy equations. Results demonstrate that an optimal fin spacing exists that balances increased surface area with sufficient space for convection currents. The 10-fin configuration achieved the highest heat transfer rate, 62% higher than the 6-fin arrangement and 18% higher than the 13-fin design. This work provides practical insights for thermal management in electronic components and demonstrates the effectiveness of the monolithic coupling approach for simulating natural convection problems.

1 Introduction

Thermal management is essential in modern electronics, as device performance, reliability, and longevity depend on effective heat dissipation. Passive cooling components like heat sinks with fin arrays are widely used due to their ability to enhance convective heat transfer by increasing surface area. In natural convection scenarios, they offer added advantages by eliminating moving parts, thus improving system reliability.

Fin array performance is influenced by buoyancy-driven flow and thermal boundary layer development, with key parameters including fin height, thickness, and spacing. When fins are too close, boundary layer merging restricts airflow, reducing efficiency. Conversely, excessive spacing lowers surface area, limiting heat dissipation. Optimal design, therefore, requires a balance.

Foundational studies by Bar-Cohen and Rohsenow proposed optimal fin spacing models for natural convection, while Elenbaas introduced empirical correlations for heat transfer in finned systems. However, precise prediction of fluid-thermal interactions remains complex.

This study uses Computational Fluid Dynamics (CFD) to simulate natural convection in fin arrays of varying configurations (6, 10, and 13 fins). The goal is to identify an arrangement that maximizes heat transfer while minimizing material usage, providing valuable insights for efficient passive cooling design.

2 Numerical Method and Simulation Design

2.1 Numerical Method

The governing equations for this problem include the conservation of mass, momentum, and energy equations, coupled through the Boussinesq approximation:

$$\nabla \cdot \mathbf{u} = 0 \quad \text{(Mass balance)} \tag{1}$$

$$\rho \left[\frac{\partial \mathbf{u}}{\partial t} + (\mathbf{u} \cdot \nabla)\mathbf{u} \right] = \mu \nabla^2 \mathbf{u} - \nabla p + \mathbf{b} \quad \text{(Momentum balance)} \tag{2}$$

$$\rho c_v \left[\frac{\partial T}{\partial t} + \mathbf{u} \cdot \nabla T \right] = K \nabla^2 T + R \quad \text{(Energy balance)} \tag{3}$$

The body force term incorporates the Boussinesq approximation:

$$\mathbf{b} = [1 - \beta(T - T_0)]\mathbf{g} \tag{4}$$

The coupling between the equations occurs in two directions:

1. The velocity field influences the convective heat transfer in the energy equation.
2. The temperature field influences the body force term in the momentum equation.

Two key dimensionless parameters characterize the flow:

$$\text{Rayleigh number based on spacing:} \quad Ra_S = \frac{g\beta(T_s - T_\infty)S^3}{\nu^2}\text{Pr} \tag{5}$$

$$\text{Rayleigh number based on height:} \quad Ra_L = \frac{g\beta(T_s - T_\infty)L^3}{\nu^2}\text{Pr} \tag{6}$$

Prandtl number:

$$\text{Pr} = \frac{\mu}{\rho K} \tag{7}$$

We employed a unified monolithic coupling approach, creating a mixed function space:

$$\mathcal{W} = \mathcal{U} \otimes \mathcal{P} \otimes \mathcal{T} \tag{8}$$

For temporal discretization, we used the θ-method with $\theta = 0.5$ (Crank–Nicolson scheme). To address instabilities in advection-dominated flows and satisfy the LBB condition, we implemented SUPG and PSPG stabilization techniques.

2.2 Simulation Design

Three different configurations were simulated, varying the number of fins while maintaining the same base dimensions:

Parameter	Configuration A	Configuration B	Configuration C
Number of fins	6	10	13
Fin spacing (mm)	17.8	9.3	6.5
Fin height (cm)	2.4	2.4	2.4
Fin thickness (mm)	5.0	5.0	5.0
Base width (cm)	14.0	14.0	14.0
Domain height (cm)	4.0	4.0	4.0

Table 1: Geometric parameters for the different fin configurations

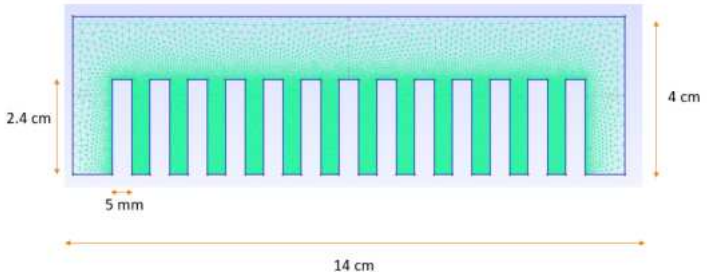

Figure 1: Computational domain showing the fin array configuration with dimensions: total width 14 cm, total height 4 cm, fin height 2.4 cm, and fin thickness 5 mm. The mesh shows triangular elements with refinement near fin surfaces.

The rectangular domain (14 cm × 4 cm) contains vertically-aligned fins (height 2.4 cm, thickness 5 mm) extending from the bottom surface. Using Gmsh, we created an unstructured triangular mesh with:

- Fin surface mesh size: 0.3 mm (for precise resolution of boundary layer effects)
- Non-fin surface mesh size: 2.5 mm (for computational efficiency in regions of less complex flow)

Element counts increased with fin density, ranging from 45,000 elements (6 fins) to 75,000 elements (13 fins).

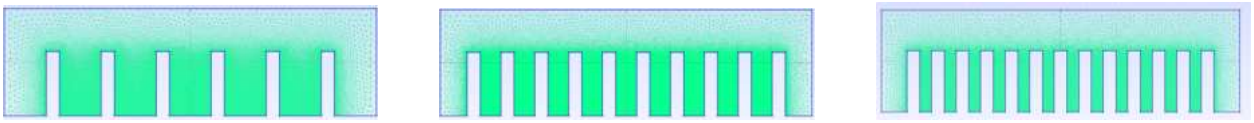

(a) Mesh for 6 fins (b) Mesh for 10 fins (c) Mesh for 13 fins

Figure 2: Computational meshes for different fin configurations

The following boundary conditions were applied:

- Bottom surface and fins: No-slip condition ($\mathbf{u} = \mathbf{0}$) and constant temperature ($T = 80C$ or 353K)
- Left, right, and top boundaries: Open boundary conditions for velocity and zero heat flux ($\nabla T \cdot \mathbf{n} = 0$)
- Initial condition: Fluid at rest ($\mathbf{u} = \mathbf{0}$) and ambient temperature ($T = 30C$ or 303K)

The physical and numerical parameters used in the simulations are summarized below:

Parameter	Value	Units
Physical properties		
Prandtl number	0.7215	-
Rayleigh number	5.69×10^8	-
Viscosity	1.847×10^{-5}	kg/(m·s)
Thermal conductivity	0.02772	W/(m·K)
Specific heat capacity	720	J/(kg·K)
Thermal expansion coefficient	1/328	K^{-1}
Gravitational acceleration	9.81	m/s^2
Numerical parameters		
Time step size	0.0275	s
Total simulation time	5	s
θ parameter	0.5	-
Newton solver tolerance	10^{-7}	-

Table 2: Physical and numerical parameters used in the simulations

The implementation utilized the DOLFINx library with a Newton solver and GMRES linear solver with LU preconditioner. The simulations were parallelized using MPI, with each simulation running on 4 processing cores.

3 Results

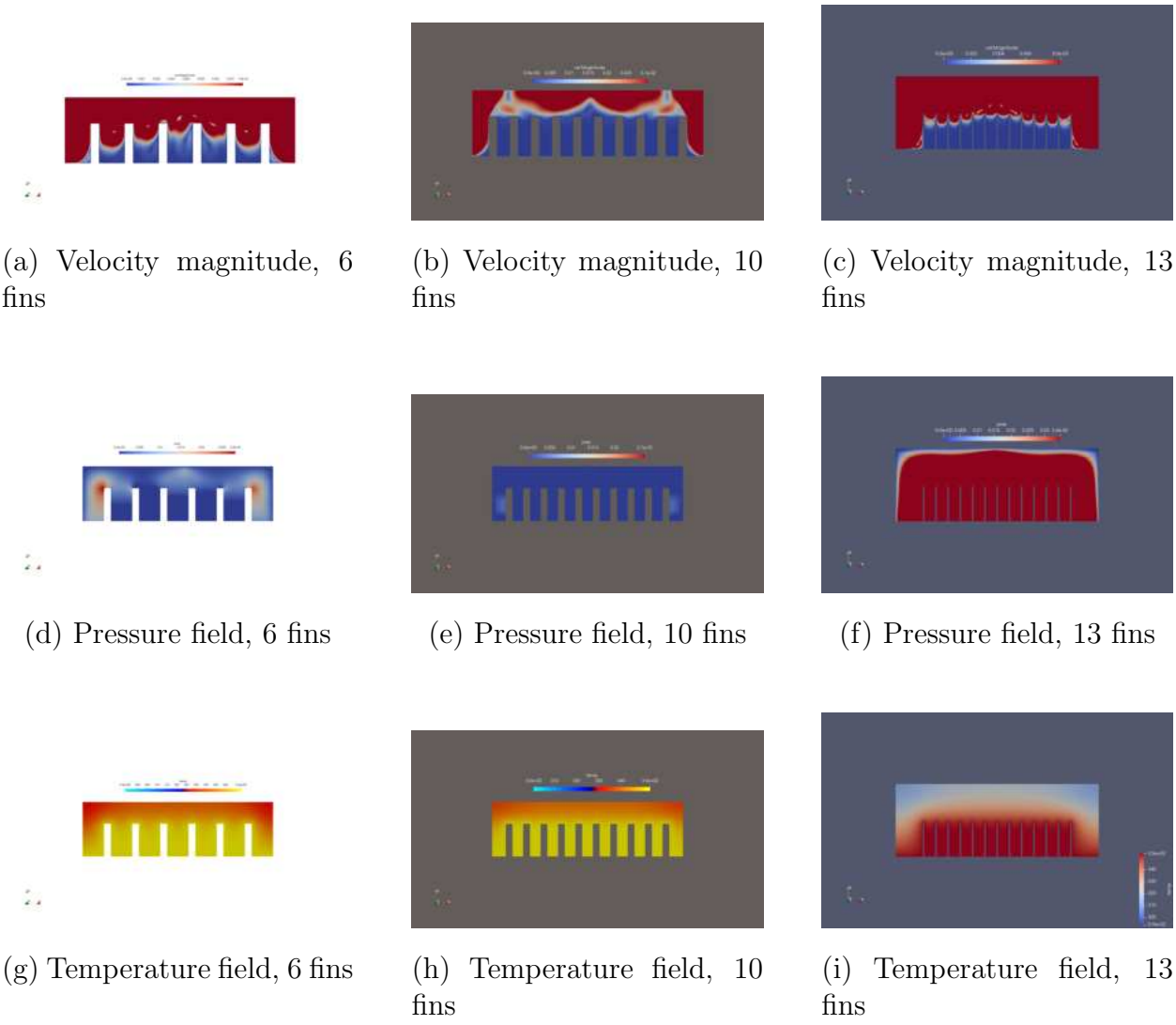

(a) Velocity magnitude, 6 fins

(b) Velocity magnitude, 10 fins

(c) Velocity magnitude, 13 fins

(d) Pressure field, 6 fins

(e) Pressure field, 10 fins

(f) Pressure field, 13 fins

(g) Temperature field, 6 fins

(h) Temperature field, 10 fins

(i) Temperature field, 13 fins

Figure 3: Simulation results at steady state (t = 5s) for different fin configurations: velocity magnitude fields (top row), pressure fields (middle row), and temperature fields (bottom row)

Figure 3 presents the pressure, velocity, and temperature fields for all three fin configurations at steady state (t = 5s). Key observations:

- **Configuration A (6 fins):**
  - Minimal pressure gradients across domain
  - Strong convection currents due to wide fin spacing
  - Effective cooling between fins but reduced overall heat dissipation

- **Configuration B (10 fins):**
  - Moderate pressure gradients creating optimal flow conditions
  - Well-developed convection currents
  - Efficient heat transfer with good penetration of cooler air
- **Configuration C (13 fins):**
  - High pressure gradients between tightly spaced fins
  - Weak convection currents due to merged boundary layers
  - Higher average temperatures between fins from restricted airflow

3.1 Temporal Evolution of Flow Patterns

Figure 4 shows the evolution of the flow field for the 10-fin configuration at three different time steps (t = 1s, t = 2.5s, and t = 5s).

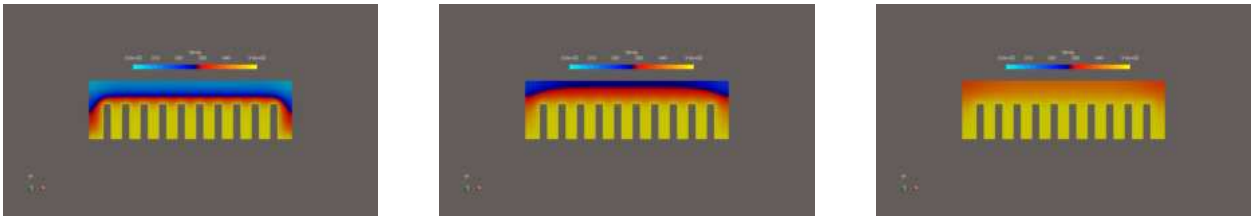

(a) t = 1s (b) t = 2.5s (c) t = 5s

Figure 4: Time evolution of flow field for the 10-fin configuration showing pressure (top row), velocity magnitude (middle row), and temperature (bottom row)

Initially (t = 1s), heat conduction dominates, with minimal pressure gradients and thermal boundary layers forming around the fins. As time progresses, buoyancy forces become more significant, and convection currents develop, accompanied by increasing pressure variations. By t = 2.5s, clear pressure gradients and thermal plumes are visible above the fin array. At t = 5s, a quasi-steady state is reached with fully developed pressure, velocity, and temperature fields.

3.2 Heat Transfer Performance

The heat transfer rate was calculated by integrating the conductive heat flux across the fin surfaces. Table 3 presents the steady-state heat transfer rates for different fin configurations. Each fin has a thickness of 5 mm.

Configuration	Number of Fins	Fin Spacing (mm)	Heat Transfer Rate (W)
A	6	17.8	2.85
B	10	9.3	4.62
C	13	6.5	3.92

Table 3: Heat transfer performance for different fin configurations

These results demonstrate that heat transfer is governed by two competing effects: buoyancy-driven enhancement with increasing fin number, and flow disruption due to excessive friction when fins are too closely spaced. Configuration B, with 10 fins, achieves the highest heat transfer rate—62% higher than Configuration A and 18% higher than Configuration C.

3.3 Boundary Layer Interaction

Analysis of the velocity profiles between fins provides insight into the boundary layer development and interaction. As shown in Figure 5, boundary layers develop at the lower end of fin surfaces and eventually merge if the spacing is sufficiently small.

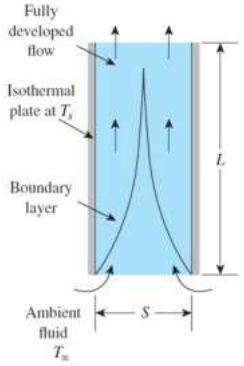

Figure 5: Velocity profiles between fins showing boundary layer interaction

The Rayleigh number based on fin spacing (Ra_S) characterizes this behavior:

Configuration	Fin Spacing (mm)	Computed Ra_S	Flow Regime
A	17.8	1.42×10^4	Isolated boundary layers
B	9.3	2.03×10^3	Interacting boundary layers
C	6.5	6.94×10^2	Merged boundary layers

Table 4: Rayleigh numbers based on fin spacing and corresponding flow regimes

Our results indicate that optimal heat transfer occurs when Ra_S is approximately in the range of 1×10^3 to 3×10^3, which corresponds to Configuration B in our study.

4 Discussion

Simulation results confirm an optimal fin spacing that maximizes natural convection by balancing surface area and airflow.

Key observations:

- **Configuration A (6 fins)**: Wide spacing allows strong airflow but limits heat transfer due to reduced surface area.
- **Configuration C (13 fins)**: High surface area but suffers from poor airflow as boundary layers merge, lowering heat transfer.
- **Configuration B (10 fins)**: Achieves the best performance by enabling partial boundary layer interaction with sufficient airflow and surface area.

These results align with the model proposed by Bar-Cohen and Rohsenow, which predicts optimal heat transfer when boundary layers just begin to interact .

5 Conclusion

This study investigated the natural convection heat transfer performance of heat sink fin arrays using computational fluid dynamics. The main conclusions are:

- **Optimal fin spacing** maximizes heat transfer by balancing surface area and airflow. Configuration B (10 fins) performed best, achieving a heat transfer rate:
  - 62% higher than Configuration A (6 fins), and
  - 18% higher than Configuration C (13 fins).
- **Thermal boundary layer interaction** is a key factor. Optimal heat transfer occurs when adjacent boundary layers just begin to interact, typically at a spacing-based Rayleigh number (Ra_S) between 1×10^3 and 3×10^3.
- The **monolithic coupling approach** effectively captured the interaction between fluid flow and heat transfer, validating its use for natural convection simulations.
- These findings have practical implications for **heat sink design in electronics**, emphasizing the importance of optimizing fin spacing rather than simply increasing fin count.

References

[1] Bar-Cohen, A., and Rohsenow, W.M., "Thermally Optimum Spacing of Vertical, Natural Convection Cooled, Parallel Plates," Journal of Heat Transfer, Vol. 106, pp. 116-123, 1984.

[2] Donea, J., and Huerta, A., "Finite Element Methods for Flow Problems," John Wiley & Sons, 2003.

[3] Bejan, A., "Convection Heat Transfer," 4th Edition, John Wiley & Sons, 2013.

[4] Elenbaas, W., "Heat Dissipation of Parallel Plates by Free Convection," Physica, Vol. 9, No. 1, pp. 1-28, 1942.

[5] Zienkiewicz, O.C., Taylor, R.L., and Nithiarasu, P., "The Finite Element Method for Fluid Dynamics," 7th Edition, Butterworth-Heinemann, 2014.

[6] Tezduyar, T.E., "Stabilized Finite Element Formulations for Incompressible Flow Computations," Advances in Applied Mechanics, Vol. 28, pp. 1-44, 1991.

[7] Logg, A., Mardal, K.A., and Wells, G.N., "Automated Solution of Differential Equations by the Finite Element Method: The FEniCS Book," Springer, 2012.

[8] Yazicioglu, A.G., and Yüncü, H., "Optimum Fin Spacing of Rectangular Fins on a Vertical Base in Free Convection Heat Transfer," Heat and Mass Transfer, Vol. 44, pp. 11-21, 2007.

[9] Culham, J.R., and Muzychka, Y.S., "Optimization of Plate Fin Heat Sinks Using Entropy Generation Minimization," IEEE Transactions on Components and Packaging Technologies, Vol. 24, No. 2, pp. 159-165, 2001.

[10] Incropera, F.P., Dewitt, D.P., Bergman, T.L., and Lavine, A.S., "Fundamentals of Heat and Mass Transfer," 7th Edition, John Wiley & Sons, 2011.